Original Article

Tumor Biology

# Intravenous miR-144 inhibits tumor growth in diethylnitrosamine-induced hepatocellular carcinoma in mice

Tumor Biology
October 2017: 1–8

DOI: 10.1177/1010428317737729
journals.sagepub.com/home/tub
SAGE

**Quan He[1], Fangfei Wang[1], Takashi Honda[1], Diana M Lindquist[2], Jonathan R Dillman[2,3], Nikolai A Timchenko[4] and Andrew N Redington[1,5]**

## Abstract

Previous in vitro studies have demonstrated that miR-144 inhibits hepatocellular carcinoma cell proliferation, invasion, and migration. We have shown that miR-144, injected intravenously, is taken up by the liver and induces endogenous hepatic synthesis of miR-144. We hypothesized that administered miR-144 has tumor-suppressive effects on liver tumor development in vivo. The effects of miR-144 on tumorigenesis and tumor growth were tested in a diethylnitrosamine-induced hepatocellular carcinoma mouse model. MiR-144 injection had no effect on body weight but significantly reduced diethylnitrosamine-induced liver enlargement compared with scrambled microRNA. MiR-144 had no effect on diethylnitrosamine-induced liver tumor number but reduced the tumor size above 50%, as evaluated by magnetic resonance imaging (scrambled microRNA 23.07 ± 5.67 vs miR-144 10.38 ± 2.62, $p < 0.05$) and histological analysis (scrambled microRNA 30.75 ± 5.41 vs miR-144 15.20 ± 3.41, $p < 0.05$). The levels of miR-144 was suppressed in tumor tissue compared with non-tumor tissue in all treatment groups (diethylnitrosamine–phosphate-buffered saline non-tumor 1.05 ± 0.09 vs tumor 0.54 ± 0.08, $p < 0.01$; diethylnitrosamine–scrambled microRNA non-tumor 1.23 ± 0.33 vs tumor 0.44 ± 0.10, $p < 0.05$; diethylnitrosamine-miR-144 non-tumor 54.72 ± 11.80 vs tumor 11.66 ± 2.75, $p < 0.01$), but injection of miR-144 greatly increased miR-144 levels both in tumor and non-tumor tissues. Mechanistic studies showed that miR-144 targets *epidermal growth factor receptor* and inhibits the downstream Src/AKT signaling pathway which has previously been implicated in hepatocellular carcinoma tumorigenesis. Exogenously delivered miR-144 may be a therapeutic strategy to suppress tumor growth in hepatocellular carcinoma.

## Keywords

miR-144, hepatocellular carcinoma, AKT signaling pathway, magnetic resonance imaging

Date received: 24 July 2017; accepted: 1 September 2017

## Introduction

Hepatocellular carcinoma (HCC) is the commonest type of liver cancer, making up 80% cases. An earlier study showed that the overall median survival rate of HCC was 11 months.[1] Liver cancer is a major contributor to both cancer incidence and mortality worldwide.[2] MicroRNAs (miRNAs) are naturally existing, small (18–24 base pairs), noncoding RNA. They universally regulate target protein levels via binding to their binding sites in the untranslated region leading to messenger RNA (mRNA) degradation and/or stop translation. Most miRNAs have multi-targets, and one gene maybe regulated by multiple miRNAs.[3] miRNA has its own coding gene and is highly regulated.[4] Dysregulation of

[1]Heart Institute, Cincinnati Children's Hospital Medical Center, Cincinnati, OH, USA
[2]Imaging Research Center, Cincinnati Children's Hospital Medical Center, Cincinnati, OH, USA
[3]Department of Radiology, Cincinnati Children's Hospital Medical Center, Cincinnati, OH, USA
[4]Division of Pediatric General and Thoracic Surgery, Cincinnati Children's Hospital Medical Center, Cincinnati, OH, USA
[5]Department of Pediatrics, University of Cincinnati, Cincinnati, OH, USA

**Corresponding author:**
Andrew N Redington, Heart Institute, Cincinnati Children's Hospital Medical Center, 3333 Burnet Avenue, Cincinnati, OH 45229-3026, USA.
Email: Andrew.redington@cchmc.org

miRNA has been associated with outcomes in multiple human diseases including cardiovascular disease, neurodegenerative diseases, and cancers.[5] Indeed, miRNAs are involved in the initiation, progression, and metastasis acting as oncogenes or tumor suppressor genes, and plasma or tumor miRNA levels have been proposed as biomarkers of diagnosis, treatment response, and prognosis.[6] In this regard, while miR-144 has been shown to promote cell proliferation in insulinomas,[7] most reports have demonstrated that miR-144 has predominant tumor-suppressant effects. For example, miR-144 inhibits proliferation in lung cancer and uveal melanoma cells by targeting the TP53-inducible glycolysis and apoptosis regulator (TIGA) and c-MET expression, respectively.[8,9] MiR-144 suppresses growth and metastasis of laryngeal squamous cell carcinoma by targeting insulin receptor substrate 1 (IRS1),[10] and miR-144 also suppresses proliferation and migration in HCC by targeting SMAD4 and E2F3.[11,12]

In a previous study from our laboratory, we showed that Cy3-labeled miR-144 administered via single-tail vein injection was rapidly taken up by the liver. Furthermore, unlabeled miR-144 levels continued to increase up to 28 days, suggesting induction of de novo synthesis.[13] We therefore tested the hypothesis that intravenous miR-144 would modify liver tumor development in intact animals. We employed a diethylnitrosamine (DEN)-induced liver tumor model in C3H mice, with assessment of tumorigenesis, tumor growth, and a candidate upstream modifier *epidermal growth factor receptor (*EGFR) signaling–mediated changes within the Src/AKT pathway.

## Materials and methods

### *Reagents*

DEN was obtained from Sigma (St. Louis, MO, USA). Pierce BCA Protein Assay Kit, Pierce ECL Western Blotting Substrate, Restore™ Western Blot Stripping Buffer, polyvinylidene difluoride (PVDF) membrane, and horseradish peroxidase (HRP)-conjugated anti-rabbit IgG were ordered from Thermo Fisher Scientific (Rockford, IL, USA). Primary antibodies against phospho-AKT (Ser473), phospho-Src (Tyr416), and β-actin were purchased from Cell Signaling Technology (Boston, MA, USA). Modified miRNA including miR-144 (5′-uaCAGUAUAGAUGAUGUAcuag-3′) and scrambled control (5′-aaGGCAAGCUGACCCUGAaguu-3′) were synthesized by Eurofins Genomics AT GmbH (Vienna, Austria). The modifications include 3′-cholesterol, 3× phosphorothioate (PTO) 3′-side, 2× PTO 5′-side, and 2′-O-methyl-RNA.

### *Western blot*

Protein was isolated after centrifugation of homogenized tissue in a lysis buffer containing 150 mM NaCl, 50 mM Tris Cl (pH 7.5), 0.5% deoxycholate, 0.1% sodium dodecyl sulfate (SDS), 1% Nonidet P-40, PhosSTOP, and Complete Mini. The protein concentration was determined with the Coomassie protein assay kit using bovine serum albumin (BSA) as the standard. Aliquots of samples (50 µg protein) were subjected to SDS–polyacrylamide gel electrophoresis (SDS-PAGE) and electro-transferred to a PVDF membrane at 35 V overnight at 4°C. The membrane was incubated in 5% nonfat milk in phosphate-buffered saline (PBS) containing 0.1% Tween 20 (PBS-T) for 1 h at room temperature and then overnight at 4°C in the same buffer containing primary antibody. The membrane was washed with PBS-T and incubated with HRP-conjugated secondary antibody at room temperature for 1.5 h. After being washed, the membrane was developed with SuperSignal West Pico Chemiluminescent reagent at room temperature. The signal was detected through an exposure to X-ray film and analyzed by scanning densitometry. The target protein was normalized to the loading control and expressed as the fold change versus the controls.

### *Stem-loop quantitative reverse transcription polymerase chain reaction*

Total RNA was extracted from RNAlater preserved tissues using TRIzol reagent, and stem-loop quantitative reverse transcription polymerase chain reaction (RT-qPCR) was carried out using TaqMan miRNA Reverse Transcription and TaqMan miRNA Assay kits according to manufacturer's instructions. MiR-144 level was determined using the ΔΔCt method[14] and expressed as relative to control, and RNA U6 (RNU6B) was used as normalizer.

### *Animal experiments*

Animal protocols were approved by the Institutional Animal Care and Use Committee of the Cincinnati Children's Hospital Medical Center. Mice were housed in a fully equipped animal facility, given free access to food and water ad libitum, and on a 12-h dark/light cycle. HCC was induced by a single-dose (1 mg/kg) DEN injection in 14-day-old C3H mice (Charles River Laboratories, Wilmington, MA, USA). For long-term studies of miR-144 on liver tumor development, miR-144 (40 mg/kg) was injected the second day post DEN injection, and the dosage was repeated every month for 9 months. The dosage of 40 mg/kg was decided empirically, but based on our previous and ongoing experiments showing no adverse effects and a significant increase in hepatic miR-144 of that dose. Injection of PBS and scrambled miRNA served as controls. A group of age-matched mice without any treatment were served as vehicle. The first dose of miR-144 was administered via intraperitoneal (IP) injection and all others were via tail vein injection. Liver tumors were assessed by magnetic resonance imaging (MRI) when the

mice turned to 9-month-old, for example, 2 weeks after the ninth injection of miRNA, and directly from photographs of the liver taken after removal 2 weeks post MRI. For an assessment of the EGFR signaling–mediated changes within the Src/AKT pathway, groups of miR-144 and PBS-injected C3H mice were sacrificed 2 weeks after the fourth injection of miRNA. A group of age-matched miR-144 knockout (KO) mice[15] were sacrificed for comparison.

### *Tail vein injection*

Mice were pre-warmed in housing cage with heat lamp for 15 min to dilate the blood vessel. Mouse was restrained in Tailveiner Restrainer from Braintree Scientific (Braintree, MA, USA). Mouse tail was swabbed with alcohol pad to increase the visibility of the vein. Less than 200 µL of miRNA was injected with BD 1 mL syringe 27G needle. The needle was removed from the vein and slight pressure was applied to the puncture site with a piece of gauze until the bleeding has stopped.

### *Liver MRI*

Mice were anesthetized with isoflurane in air and positioned on a bed equipped with a nose cone for anesthesia delivery. The bed was centered inside a 38-mm linear coil (Bruker, Ettlingen, Germany), which was positioned at isocenter in a 7T Bruker Biospec horizontal bore MRI scanner. Temperature and respiration were monitored using equipment from Small Animal Instruments, Inc (SAII, Stony Brook, NY, USA), and mice were kept warm with a flow of heated air through the magnet bore. Axial T2-weighted images were acquired using a fast spin-echo sequence with a repetition time of 2600 ms and an effective echo time of 45.5 ms using an in-plane resolution of $125 \times 200$ µm and a slice thickness of 750 µm. Coronal T2-weighted images were acquired using a fast spin-echo sequence with a TR of 2000 ms and an effective echo time of 32.5 ms using an in-plane resolution of $200 \times 200$ µm and a slice thickness of 750 µm.

### *Tumor quantification*

The number of liver tumors was counted by blinded observers, based on abdominal MRI images following general clinical diagnostic standards. Large tumors may be shown on several images but were only counted once. Tumor area was measured from MR images using ImageJ. The sum total of tumor area was divided by that of liver area and expressed as percent of liver area. The tumor number and size were also calculated based on liver pictures obtained when the animals were sacrificed by end of the experiments. The tumor number was counted based on visual observation from pathology specimens. The tumor size was calculated based on front and back pictures of the liver specimen and expressed as percent of liver area in the same way as MRI image analysis. The tumor number and size were presented as an average of blind analyzed data from two trained scientists.

### *Statistical analysis*

Data are expressed as means ± standard error (SE). Differences in mean values were analyzed by a two-tailed *t*-test. The $p$ values $< 0.05$ were considered significant.

## Results

### *DEN-induced HCC*

To test the effects of miR-144 on liver tumor development, we employed hepatocellular tumor mouse model induced by single-dose DEN injection. Age- (14-day-old) and body-weight- (around 8 g) matched 35 C3H mice were injected DEN via IP. Each four mice of groups PBS and miR-144 injection were sacrificed at 4 months post the fourth injection of miRNA for mechanistic study. The rest of the mice of groups PBS (8), SCR (8), and miR-144 (11) were survived till end of the experiment (9-month-old post ninth miRNA injection). As shown in Figure 1(a)–(d), all the survival mice developed HCC. In contrast to not much effect on body weight (Figure 1(e)), kidney weight (Figure 1(f)), and heart weight (Figure 1(g)), DEN injection dramatically increased liver weight (Figure 1(h)) compared with vehicle. MiR-144 significantly reduced DEN-induced liver enlargement compared with SCR or PBS controls (Figure 1(h)) indicating DEN-specific target to liver and miR-144-potentiated hepatic effects of DEN.

### *MiR-144 decreases tumor burden in DEN-induced HCC*

To evaluate the tumor development non-invasive in DEN-injected mice, we employed MR imaging by end of the experiment (9-month-old). The respective images are shown in Figure 2(a) and the quantified data are shown in Figure 2(b) and (c). MiR-144 has no effect on tumor number but significantly decreased tumor size above 50% compared with either PBS or SCR groups (Figure 2(c)). Though MRI has advantages regarding to detect liver tumors noninvasively, but limited by its sensitivity on smaller tumors. By end of the experiments, livers were extracted and imaged on both sides. The tumor number and size were evaluated using ImageJ software. As shown in Figure 2(d), miR-144 treatment group showed small tumor compared with PBS and SCR groups. The number and size were quantified in Figure 2(e) and (f). Highly consistent with MRI results, miR-144 had no effect on tumor number but significantly decreased tumor size (Figure 2(e) and (f)).

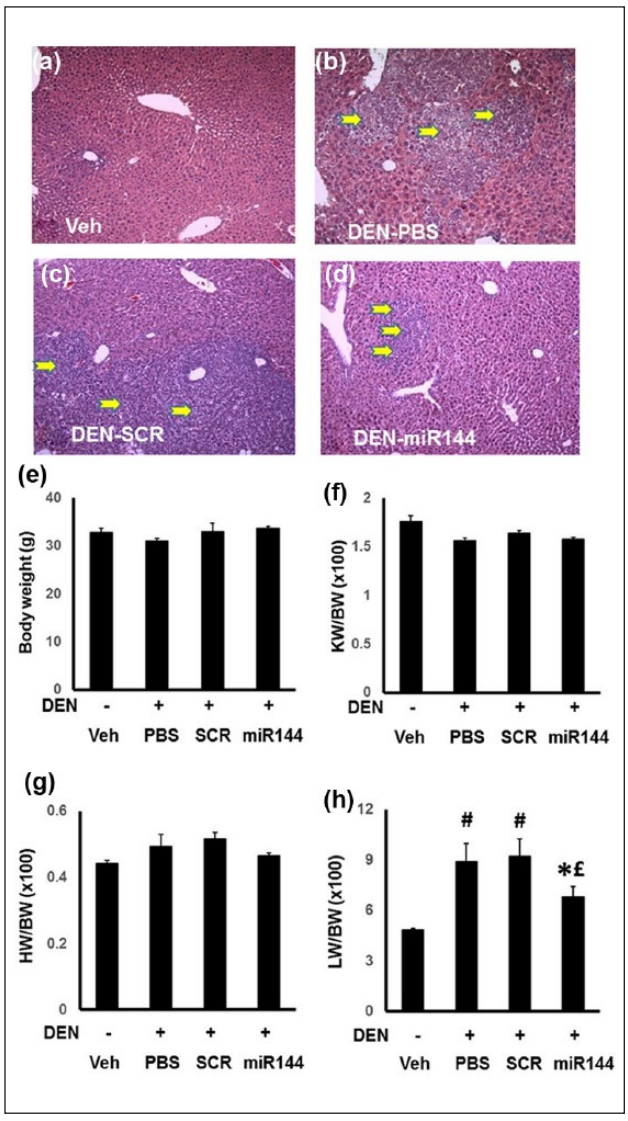


**Figure 1.** Effects of miR-144 on DEN-induced hepatocellular carcinoma mice. H&E stain shows DEN-induced hepatocellular carcinoma. Images represent pictures from (a) 7 mice of vehicle, (b) 8 mice of DEN-PBS, (c) 8 mice of DEN-SCR, and (d) 11 mice of DEN-miR-144. Arrows indicate the hepatocellular tumors. (e). Body weight. (f) Kidney weight and body weight ratio. (g) Heart weight and body weight ratio. (h) Liver weight and body weight ratio. Data represent mean ± SE from 7 mice for vehicle, 8 for DEN-PBS and DEN-SCR, and 11 for DEN-miR-144. $^{*}p < 0.05$ compared with Veh, $^{\#}p < 0.01$ compared with Veh, and $^{£}p < 0.05$ compared with DEN-PBS and DEN-SCR.

### *MiR-144 is decreased in HCC*

Decreased mature miRNA is often seen in human malignancies.[16] As determined by stem-loop qPCR, miR-144 was significantly decreased in the liver tumor compared with paired non-tumor tissue from all the treatment groups (Figure 3); however, miR-144 injection led to supra-normal levels in both tumor and adjacent normal liver.

### *MiR-144 targets EGFR/Src/AKT axis*

We employed both upregulated and downregulated miR-144 animal models to investigate miR-144 targeting signaling pathways. As shown in Figure 4(a) and (b), tail vein injection of miR-144 increased liver miR-144 level by 15-fold compared with PBS, but the liver miR-144 level was decreased by 95% in miR-144 KO mice compared with wild-type littermates. MiR-144 injection knocked down Src activity in the liver, but phosphorylated Src was significantly increased in miR-144 KO mice liver (Figure 4(c) and (d)). AKT regulates diverse cellular process including cell proliferation/survival/apoptosis, energy metabolism, angiogenesis, and stress responses. It has been postulated as a target for cancer therapy and a variety of AKT inhibitors are being tested in clinical trials.[17] To assess the effects of miR-144 on the Src/AKT pathway in the liver, we measured levels of its downstream mediator, activated AKT, which was reduced by miR-144 injection, but significantly induced in miR-144 KO mice (Figure 4(e) and (f)), suggesting that miR-144 targets the Src/AKT signaling pathway. The EGFR/Src/AKT signaling axis has been shown to modulate self-renewal of stem-like side-population cells in non-small-cell lung cancer.[18] When searching for putative upstream targets of the Src/AKT signaling pathway, we found conserved miR-144 binding site in the 3′-untranslated region of EGFR mRNA (Figure 4(g)). MiR-144 knocked down liver EGFR in miR-144-injected mice, but it was significantly induced in miR-144 KO liver (Figure 4(h) and (i)). In summary, miR-144 targets EGFR by knocking down EGFR/Src/AKT axis.

## Discussion

### *DEN-induced HCC*

The induction of HCC by DEN is well documented, and our current data demonstrated that DEN specifically induced liver enlargement without affecting animal growth indicated by body weight, kidney, and heart. Consistent with previous reports,[19] our data also confirmed that C3H mice are very sensitive to the effects of DEN, even 1 mg/kg being sufficient to induce HCC. The disadvantage of the DEN-induced HCC model is the long time period, up to 9 months, between treatment and overt disease. Nonetheless, our data showed a highly consistent tumor burden, when assessed by MRI and histological measurements at the end of the experiment. Although chemically induced mouse liver tumors are considered relatively resistant to treatment,[20] our data showed miR-144 effectively suppressed growth of HCC induced by DEN, providing a potential new avenue for liver cancer therapy.

### *MiR-144 slows HCC growth*

Our study shows that miR-144 treatment does not affect tumor number, but significantly reduces tumor size

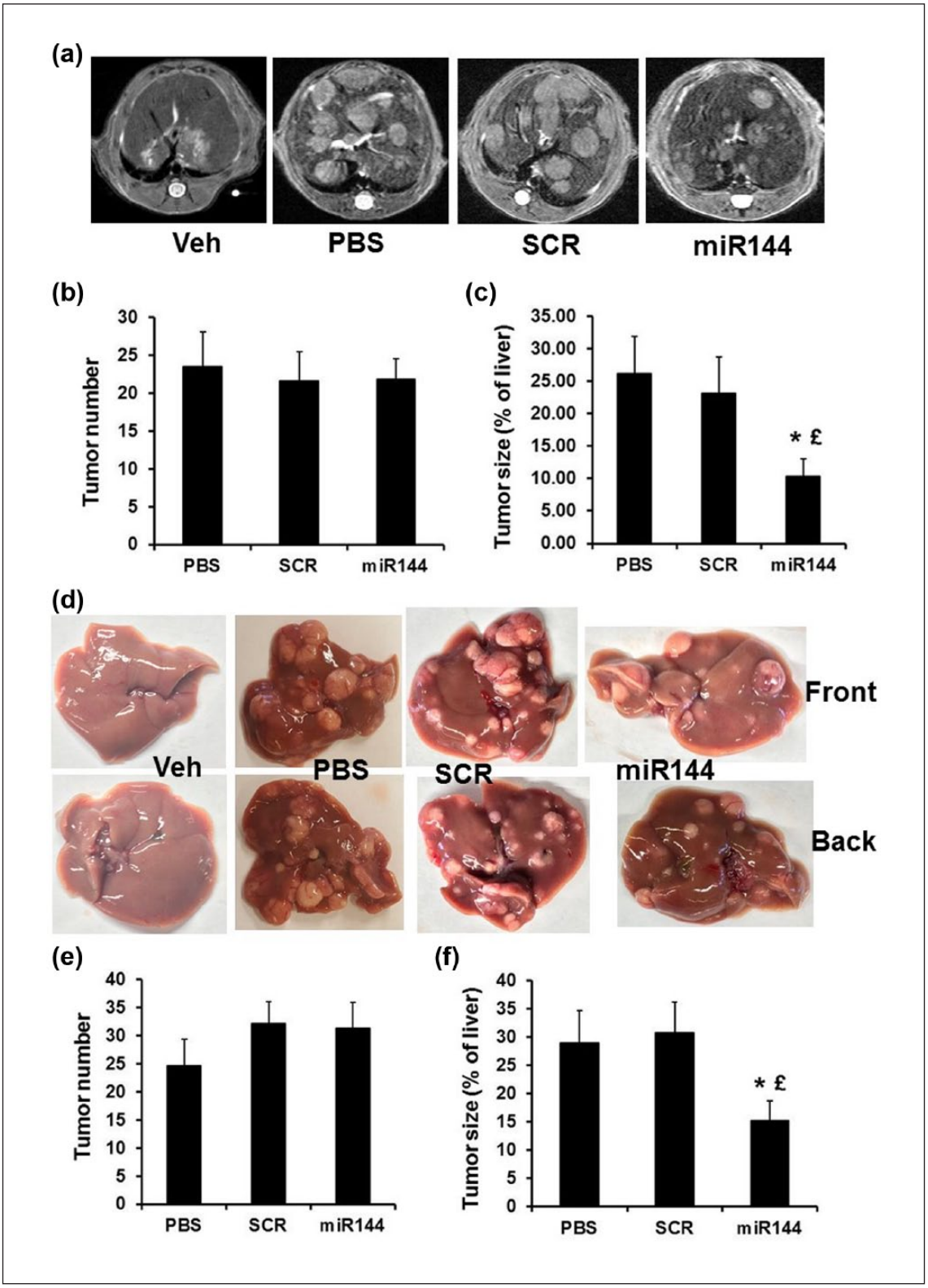


**Figure 2.** MiR-144 slows tumor growth. The development of liver tumor was evaluated by MRI and histological analysis at the end of the experiment. (a) Tumors over 0.5 × 0.5 mm are detectable. (b and e) The tumor number and (c and f) size were determined using ImageJ based on the MRI images. (d) At the end of the experiment, the liver was removed and photographed for tumor analysis. The tumor size represented by area expressed as percent of liver was determined by ImageJ. $^{*}p < 0.05$ compared with PBS and $^{£}p < 0.05$ compared with SCR treatment. $N = 8$ for PBS and SCR groups and $N = 11$ for miR-144 treatment group.

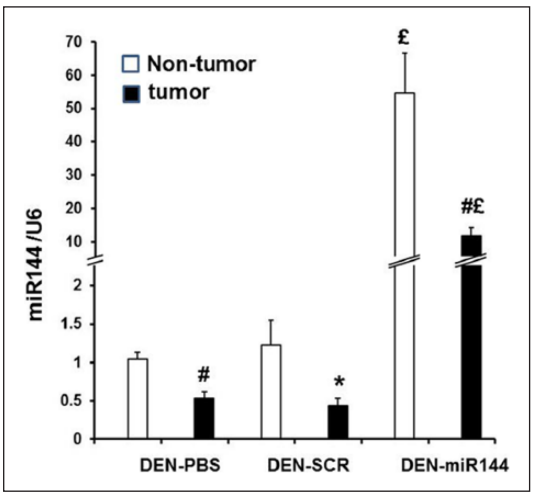


**Figure 3.** MiR-144 levels in tumor and non-tumor tissues. Total RNA was isolated from tumor and non-tumor tissues and miR-144 was determined by stem-loop RT-qPCR. MiR-144 is decreased in tumor tissue compared with non-tumor tissue in all treatment groups, but was clearly 'rescued' by miR-144 injection. $^{*}p < 0.05$ and $^{\#}p < 0.01$ compared with non-tumor tissue and $^{£}p < 0.01$ compared with DEN-PBS or DEN-SCR. $N = 5$ for each treatment group.

approximately 9 months after DEN-induced development of HCC (Figure 2). This novel in vivo data, using intravenously administered miR-144, is compatible with prior data in HCC cell lines transfected with miR-144, showing inhibition of cell proliferation, invasion, and migration. Several other studies have shown significant effects of miR-144 on tumorigenesis, albeit via targeting different pathways. For example, in lung cancer models, miR-144 suppresses tumor growth and metastasis by targeting zinc finger X-chromosomal protein,[21] TIGAR,[9] or activating protein 4.[22] MiR-144 was also demonstrated to be tumor-suppressive in papillary thyroid cancer by directly targeting E2F8.[23] The tumor-suppressive effects of miR-144 have also been demonstrated in colorectal cancer,[24] breast cancer,[25] bladder cancer,[26] uveal melanoma,[8] and squamous cell carcinoma.[10]

## *MiR-144 suppression in tumor tissue*

Lower levels of miR-144 in tumors are associated with accelerated growth and increased metastatic potential. Our data showed that miR-144 level was decreased in tumor tissue compared with non-tumor tissue (Figure 3), and this

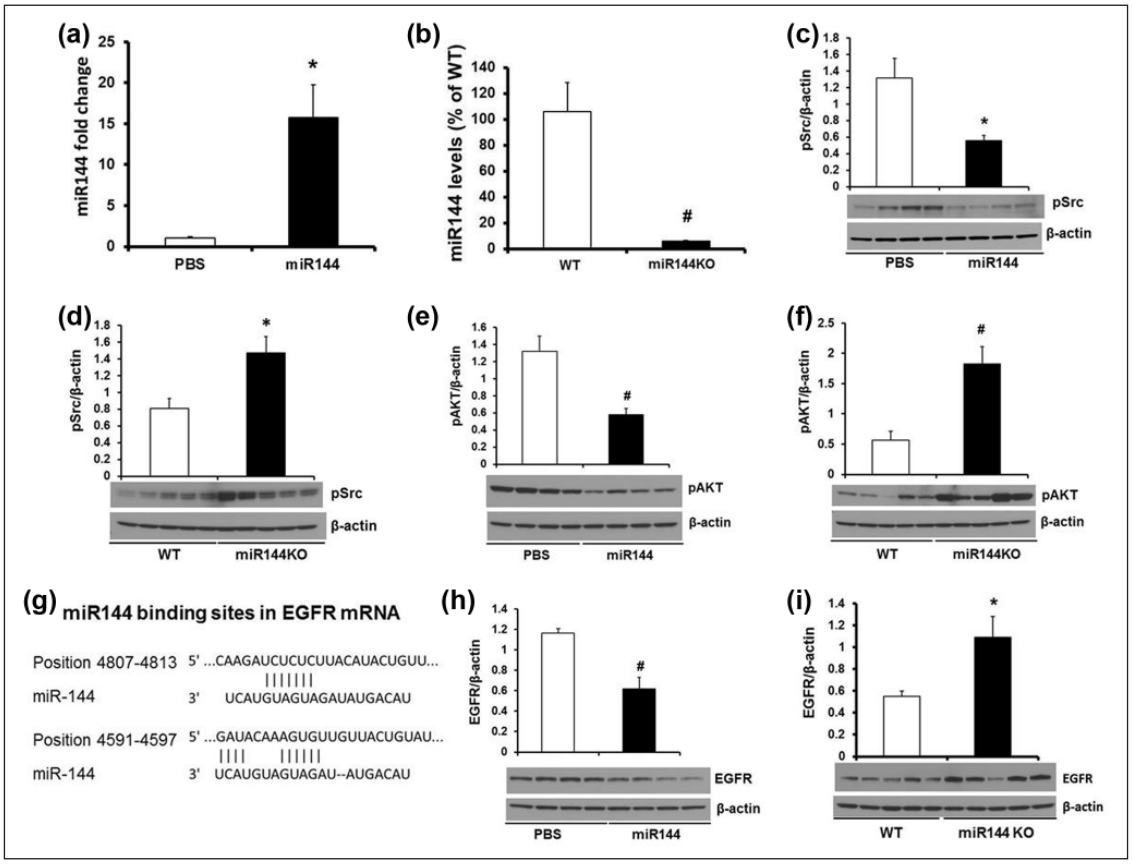


**Figure 4.** MiR-144 target EGFR/Src/AKT axis. Tail vein injection of miR-144 (a) increases liver miR-144, (c) decreases Src phosphorylation, (e) decreases AKT phosphorylation and (h) decreases EGFR protein, while miR-144/451 KO (b) decreases liver miR-144, (d) increases Src phosphorylation, (f) increases AKT phosphorylation, (g) illustration of the preserved miR-144 binding sites on the 3'-untranslated region of EGFR mRNA, and (i) increases EGFR protein. Data represent mean ± SE from four mice from PBS and miR-144 injection groups and five mice for WT and miR-144 KO groups. $^{*}p < 0.05$ and $^{\#}p < 0.01$ compared with PBS injection or WT littermates.

is consistent with a previous study showing generally lower levels of 217 studied miRNAs in 334 human tumor samples compared with paired normal tissue.[27] The restoration of miR-144 levels in tumor tissue, following intravenous therapy, suggests that tumor cells are able to take up exogenous miR-144, but to a lesser extent than normal tissue. This 'rescue' of miR-144 levels appears to be sufficient to suppress tumor growth, although because of the nature of our study, we are unable to comment on dose-response or optimal levels, for example. Nonetheless, we believe our study to be the first to demonstrate the effects of exogenously delivered miRNA on tumor growth in vivo and as such opens a potential therapeutic avenue. While speculative, it may be that HCC is particularly suited to such therapy. We have previously shown that injection of labeled miR-144 is not only preferentially taken up in the liver, compared with other organs, but also seems to induce de novo synthesis of endogenous miR-144 for up to 28 days after a single dose.[13]

### *MiR-144 and EGFR/Src/AKT signaling axis*

Our data showed that miR-144 targets the EGFR/Src/AKT axis (Figure 4), several components of which have been individually implicated in tumorigenesis. Overexpression of human c-SRC in transgenic mice increases tumor formation, including HCC by three-fold.[28] AKT inhibition has been identified as a cancer therapeutic target for decades, although AKT kinases regulate diverse cellular processes including protein synthesis, cell survival, proliferation, and metabolism resulting in potential off-target effects.[17] Lanaya et al.[29] reported that EGFR has a tumor-promoting role in liver macrophage during HCC formation, increased expression of EGFR has been found in HCC cell lines, and transgenic mice overexpressing EGF have a higher incidence of HCC.[30] When searching for possible upstream mediators of Src, we found that EGFR is a highly conserved miR-144 target (Figure 4(g)) and subsequently that miR-144 decreased the protein level of EGFR. In contrast, miR-144 knock outs had markedly increased hepatic EGFR levels (Figure 4(h) and (i)).

In summary, while our data show a clear tumor-suppressant effect of miR-144, they are necessarily incomplete in this 'proof-of-principle' study. Further studies will be required to understand more completely the biology of miR-144 and its potential role as a therapeutic agent.

## Declaration of conflicting interests

The author(s) declared no potential conflicts of interest with respect to the research, authorship, and/or publication of this article.

## Funding

The author(s) received no financial support for the research, authorship, and/or publication of this article.

## References

1. Greten TF, Papendorf F, Bleck JS, et al. Survival rate in patients with hepatocellular carcinoma: a retrospective analysis of 389 patients. *Br J Cancer* 2005; 92: 1862–1868.
2. McGlynn KA and London WT. The global epidemiology of hepatocellular carcinoma: present and future. *Clin Liver Dis* 2011; 15: 223–243.
3. Hashimoto Y, Akiyama Y and Yuasa Y. Multiple-to-multiple relationships between microRNAs and target genes in gastric cancer. *Plos One* 2013; 8: e62589.
4. Ha M and Kim VN. Regulation of microRNA biogenesis. *Nat Rev Mol Cell Biol* 2014; 15: 509–524.
5. Das J, Podder S and Ghosh TC. Insights into the miRNA regulations in human disease genes. *BMC Genomics* 2014; 15: 1010.
6. Peng Yac MC. The role of microRNAs in human cancer. *Signal Transduct Target Ther* 2016; 1: 9.
7. Jiang X, Shan A, Su Y, et al. miR-144/451 promote cell proliferation via targeting PTEN/AKT pathway in insulinomas. *Endocrinology* 2015; 156: 2429–2439.
8. Sun L, Bian G, Meng Z, et al. MiR-144 inhibits uveal melanoma cell proliferation and invasion by regulating c-Met expression. *PLoS One* 2015; 10: e0124428.
9. Chen S, Li P, Li J, et al. MiR-144 inhibits proliferation and induces apoptosis and autophagy in lung cancer cells by targeting TIGAR. *Cell Physiol Biochem* 2015; 35: 997–1007.
10. Wu X, Cui CL, Chen WL, et al. MiR-144 suppresses the growth and metastasis of laryngeal squamous cell carcinoma by targeting iRS1. *Am J Transl Res* 2016; 8: 1–11.
11. Cao T, Li H, Hu Y, et al. MiR-144 suppresses the proliferation and metastasis of hepatocellular carcinoma by targeting E2F3. *Tumour Biol* 2014; 35: 10759–10764.
12. Yu M, Lin Y, Zhou Y, et al. MiR-144 suppresses cell proliferation, migration, and invasion in hepatocellular carcinoma by targeting SMAD4. *Onco Targets Ther* 2016; 9: 4705–4714.
13. Li J, Cai S, Peng J, et al. Time dependent distribution of microRNA 144 after intravenous delivery. *Microrna* 2016; 5: 36–49.
14. Winer J, Jung CK, Shackel I, et al. Development and validation of real-time quantitative reverse transcriptase-polymerase chain reaction for monitoring gene expression in cardiac myocytes in vitro. *Anal Biochem* 1999; 270: 41–49.
15. Wang X, Zhu H, Zhang X, et al. Loss of the miR-144/451 cluster impairs ischaemic preconditioning-mediated cardioprotection by targeting Rac-1. *Cardiovasc Res* 2012; 94: 379–390.
16. Gurtner A, Falcone E, Garibaldi F, et al. Dysregulation of microRNA biogenesis in cancer: the impact of mutant p53 on Drosha complex activity. *J Exp Clin Cancer Res* 2016; 35: 45.
17. Nitulescu GM, Margina D, Juzenas P, et al. Akt inhibitors in cancer treatment: the long journey from drug discovery to clinical use (Review). *Int J Oncol* 2016; 48: 869–885.
18. Singh S, Trevino J, Bora-Singhal N, et al. EGFR/Src/Akt signaling modulates Sox2 expression and self-renewal of stem-like side-population cells in non-small cell lung cancer. *Mol Cancer* 2012; 11: 73.
19. Lee GH, Nomura K, Kanda H, et al. Strain specific sensitivity to diethylnitrosamine-induced carcinogenesis is

maintained in hepatocytes of C3H/HeN in equilibrium with C57BL/6N chimeric mice. *Cancer Res* 1991; 51: 3257–3260.
20. Braeuning A, Bucher P, Hofmann U, et al. Chemically induced mouse liver tumors are resistant to treatment with atorvastatin. *BMC Cancer* 2014; 14: 766.
21. Zha W, Cao L, Shen Y, et al. Roles of Mir-144-ZFX pathway in growth regulation of non-small-cell lung cancer. *Plos One* 2013; 8: e74175.
22. Gao F, Wang T, Zhang Z, et al. Regulation of activating protein-4-associated metastases of non-small cell lung cancer cells by miR-144. *Tumour Biol*. Epub ahead of print 8 August 2015. DOI: 10.1007/s13277-015-3866-4.
23. Sun J, Shi R, Zhao S, et al. E2F8, a direct target of miR-144, promotes papillary thyroid cancer progression via regulating cell cycle. *J Exp Clin Cancer Res* 2017; 36: 40.
24. Iwaya T, Yokobori T, Nishida N, et al. Downregulation of miR-144 is associated with colorectal cancer progression via activation of mTOR signaling pathway. *Carcinogenesis* 2012; 33: 2391–2397.
25. Pan Y, Zhang J, Fu H, et al. MiR-144 functions as a tumor suppressor in breast cancer through inhibiting ZEB1/2-mediated epithelial mesenchymal transition process. *Onco Targets Ther* 2016; 9: 6247–6255.
26. Guo Y, Ying L, Tian Y, et al. MiR-144 downregulation increases bladder cancer cell proliferation by targeting EZH2 and regulating Wnt signaling. *FEBS J* 2013; 280: 4531–4538.
27. Lu J, Getz G, Miska EA, et al. MicroRNA expression profiles classify human cancers. *Nature* 2005; 435: 834–838.
28. Kline CL, Jackson R, Engelman R, et al. Src kinase induces tumor formation in the c-SRC C57BL/6 mouse. *Int J Cancer* 2008; 122: 2665–2673.
29. Lanaya H, Natarajan A, Komposch K, et al. EGFR has a tumour-promoting role in liver macrophages during hepatocellular carcinoma formation. *Nat Cell Biol* 2014; 16: 972–977.
30. Borlak J, Meier T, Halter R, et al. Epidermal growth factor-induced hepatocellular carcinoma: gene expression profiles in precursor lesions, early stage and solitary tumours. *Oncogene* 2005; 24: 1809–1819.